

TECHNICAL APPLICATION OF PETROLEUM LOGGING INSTRUMENTS IN MARINE LOGGING

Caiyun Gu

Peng Zhao

Li Wang

Hongxia Guo

Yulin University, Shaanxi, China

ABSTRACT

To solve the problem of offshore oilfield development, based on the newly introduced pulsed neutron oxygen activation logging instrument, the application research of test design and interpretation method was carried out and applied to actual production. The structure, technical indicators and logging principles of pulsed neutron oxygen activation logging tools were introduced. The test design under different well conditions was studied, including general positive and negative injection, oil sleeve injection, single oil pipe configuration and multi-tubing configuration. A large amount of field test data was collected and analysed technically. A set of effective interpretation models was proposed. The corresponding interpretation software was developed. A set of test design methods and operating specifications for different well conditions were developed. Based on the conventional interpretation method, the peak selection, the double-tuber peak identification and the carbon dioxide flooding interpretation method were added. The results show that the test design and interpretation methods were applied well through a large number of field tests and production applications. Therefore, pulsed neutron oxygen activated injection profile logging technology is successfully applied in offshore oil fields.

Keywords: oil logging instrument, pulsed neutron oxygen activation, injection profile logging, application

INTRODUCTION

Oil logging can provide an effective basis for the exploration and development of petroleum resources, which runs through the whole process of oil well drilling to oil well production. Therefore, the application of logging tools directly affects oil exploration and development. To improve the level of oil logging and ensure the efficient development of petroleum resources, advanced technology should be applied in the logging process.

In the process of oil and gas field exploration and development, the continuous development of logging technology has become an important "helper" for the petroleum industry personnel to qualitatively and quantitatively evaluate oil and gas reservoirs. According to various logging principles, successful oil logging tools can be used to better understand the formation. Electromagnetic

flowmeters and ultrasonic flow have been used in other industries for many years, and the logging industry has been introduced for several years, but the application effect has not been very satisfactory. For example, the electromagnetic flowmeter can only measure the liquid flow rate of the conductive medium and cannot measure the flow rate of the non-conductive medium, and the sensor material problem of the ultrasonic flow meter. Those factors hinder its development. In addition, although turbine flow, ultrasonic flow, and electromagnetic flow logging techniques are relatively advanced, they are all contact flow logging devices that require downhole contact with the test fluid. Therefore, the loop and the flow outside the tube cannot be measured. The oilfield injection well has the characteristics of long section, large number of layers and small injection volume. Most of the logs are layered or multi-tube dispensing structures. Contact measurement method cannot play a full role in complicated

wells such as stratified water injection and multi-string water injection. Logging techniques such as well temperature and noise cannot quantitatively determine the flow rate, and the injection flow logging cannot be completed separately.

The pulsed neutron oxygen activation logging method is a nuclear logging method. The water flow is activated by a pulsed neutron tube, and the water flow velocity is determined by measuring the time that the activated water flow flows through the respective detectors to determine the injection amount. The logging method uses any radiotracer. There are no problems such as contamination, sedimentation and pollution. The measurement results are not affected by lithology and pore permeability parameters and the size of the perforation diameter. It is not only suitable for the measurement of polymer injection, ternary composite solution wells, but also for the measurement of general positive injection wells, general reverse injection wells, oil casing injection wells and layered injection wells. The method can determine the flow of fluid in the tube, outside the tube and in the annulus without direct contact with the fluid and can simultaneously measure the upper and lower streams. The field is quickly and intuitively explained, and the flow rate of the measuring point can be quickly obtained. Therefore, the oil field injection profile test is widely used.

STATE OF THE ART

At present, there are two types of non-renewable energy that people use most in their daily lives. One is natural gas and the other is oil. Over time, energy is being mined frequently, which has led to a decline in global oil and gas resources reserves. However, the demand for natural gas and oil is rising. For these reasons, scientists around the world are constantly exploring new oil and gas fields, and also increasing the exploration of high-tech exploration in oil and gas fields.

The distinctive feature of the product in 2004 is that on the basis of the four-shot and double-receiving symmetric distribution products, a set of emission spacing is added to form a six-shot double of T5---T3--T1-RR-T2--T4---T6. A symmetrically distributed antenna array is received. The operating frequency is still dual frequency: 400kHz and 2MHz. An apparent resistivity curve of 12 different depths of detection is obtained, which provides a wealth of formation information. Based on a study, a typical representative of this generation of products is Weatherford's MFR [1].

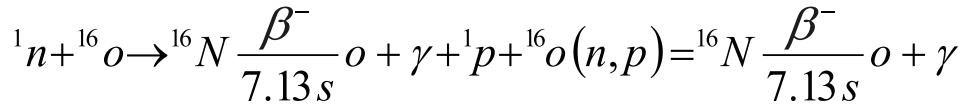
In 2005, a scholar introduced a new logging while drilling tool, that is, a directional electromagnetic logging tool. This generation of instruments mainly focuses on the depth and orientation of the instrument and optimizes the application effect in geo steering. The new directional electromagnetic wave LWD instrument uses tilt and lateral antennas with multiple source distances and frequencies to collect data as much as possible. The symmetry of the measurement makes the response sensitive to the distance to the interface and the resistivity contrast. It is not affected by resistivity anisotropy and relative tilt. In order to facilitate real-time decision making, real-time inversion software was developed [2].

In 2011, the SWFL-A pulse neutron oxygen activated water flow logging tool has been greatly upgraded and improved in technical design and performance indicators. The utility model has the advantages of various functions, simple and compact structure, various combination modes, large source distance and measurement range, higher precision, wider temperature range, reliability and convenience. The SWFL-B neutron oxygen activated water flow logging tool fully possesses the neutron lifetime logging function in the measurement function. In the neutron lifetime logging mode, the method of measuring the variable period neutron decay time spectrum of the equal width gate is adopted, and the equal-width neutron decay time spectrum is used [3].

In 2007, a scholar proposed a continuous measurement velocity model and a pulse measurement velocity model. During the measurement process, the pulsed neutron tube continuously emits a high-energy fast neutron pulse to activate the oxygen element in the fluid. The flow rate of the fluid can be determined based on the count rate measured by the instrument and the characteristic exponential decay rate [4].

PULSED NEUTRON OXYGEN ACTIVATION LOGGING

Oxygen activated water flow logging methods were proposed from the 1960s and 1970s. Until recently, a method for measuring the amount of water absorbed by each layer in a water injection well or an injection well was applied. This method is a non-contact measurement method that utilizes the activation reaction of fast neutrons to the surrounding medium. The principle is as follows: the neutron generator emits a fast neutron of 14 MeV, radiates the material around the wellbore and in the formation, and generates a radiation reaction, which can activate elements such as O, Si, and Al to generate a radioactive element with a half-life of seconds to a grade. After the reaction, ^{16}O was converted to ^{16}N (half-life 7.13S), ^{28}Si was converted to ^{28}Al (half-life 2.24min), and ^{27}Al was converted to ^{27}Mg (half-life 9.46min). All three radioactive elements emit high-energy β and γ rays. The β ray is easily absorbed by the formation rock, the surrounding medium and the logging steel shell, while the γ ray can be detected by the γ detector [5]. According to research, the oxygen nucleus produces a nitrogen isotope at 10 MeV of fast neutron activation, and the radioactive nitrogen isotope undergoes β decay with a half-life of 7.13S [6]. High energy γ rays are emitted after β decay. The energy is 6.13 MeV of radiation. The threshold energy of the ^{16}O reaction was 10.2 MeV. Therefore, the 14MeV neutron generator is suitable. Due to the high energy, 6.13 MeV γ rays can penetrate wellbore materials of several tens of centimetres, such as well fluids, tubing, casing, cement, etc. The Monte Carlo method can be used to calculate the activation profile of oxygen activation and the response function of the detector, so it is possible to predict the change in the detector count rate caused by water flow [7]. Study showed the reaction process of oxygen activation is as follows [8].



(1)

Pulsed oxygen activated water flow logging was proposed by Schlumberger in the United States in 1991 to detect vertical water flow and provide quantitative measurements of water flow velocity and flow, known as WFL logging methods.

When logging, the generator hits the neutron for a few seconds. The surrounding water is activated. Then, after a few seconds of rest, several detectors simultaneously record the time spectrum of the γ signal. If the water is flowing, after a period, the water reaches the detectors in turn, and a peak appears in the time spectrum of each detector. According to the position of the peak on the time spectrum, the time T of the water flow reaching each detector is known, and the distance travelled by the water during this time is the source distance L of each detector, and the speed of the water is $V=L/T$. Since the borehole and the tubing diameter D are known, the cross-sectional area S of the water can be calculated, and the flow rate $Q = VS$ [9].

If the neutron pulse time width is T_a , the time that the activated water flows from the neutron source to the detector can be obtained by the following equation [10]:

$$T_m = \frac{T_a}{2} + \frac{\int f(t)tdt}{\int f(t)dt} \quad (2)$$

INTERPRETATION AND APPLICATION OF PULSED NEUTRON OXYGEN ACTIVATION LOGGING

FEATURE ANALYSIS OF SPECTRAL PEAK RECOGNITION

The time peaks recorded by the pulsed neutron oxygen activation log show different forms with the flow velocity of the measured fluid. The spectral peak characteristics are generally described in terms of the amplitude, width and symmetry of the peak [11].

A single peak characteristic is produced when there is only one column space fluid flow at the measurement site. A single peak characteristic is also produced when the fluid flow direction and flow rate in the two column spaces are exactly the same, which is a special case. In actual production, it rarely happens.

The bimodal and the two peaks appear as a superposition of two single peaks on the time spectrum. According to the degree of overlap, it can be divided into non-overlapping, partial overlap and severe overlap. This situation is the performance of two kinds of column space fluid flow at the measuring point [12]. For example, the tubing and the loop space have fluids that flow simultaneously downward [13].

First, the non-overlapping bimodal. There is a significant bimodal on the time spectrum, and the points between the two peaks are more open. There is no overlap.

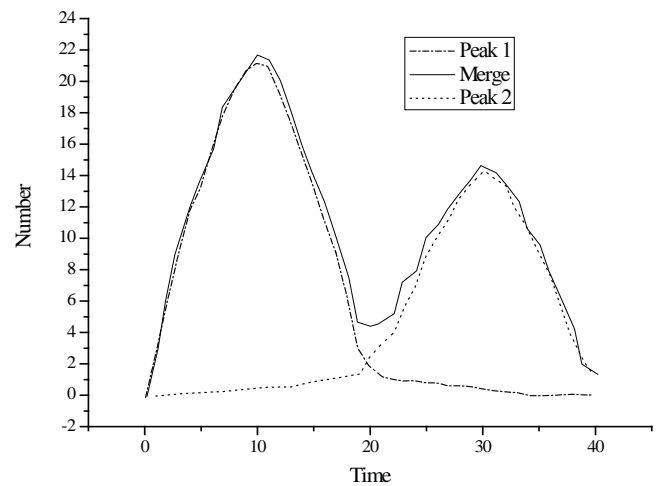


Fig. 1. Theoretical graph of non-overlapping bimodal

Second, partially overlapping bimodal. The time spectrum is shown as two peaks, and the lower half of the single peak overlaps.

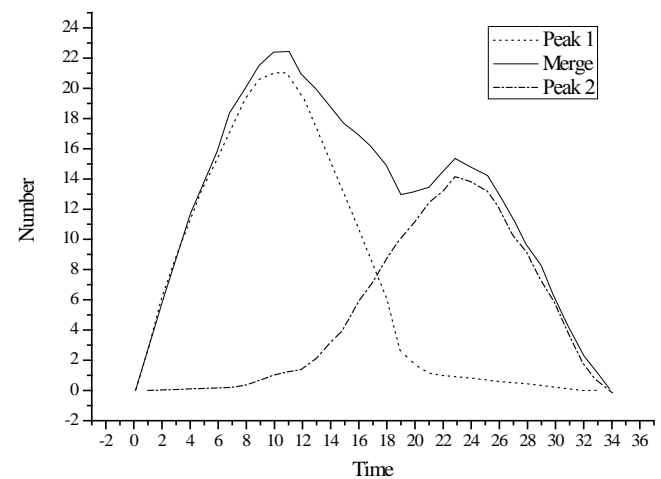


Fig. 2. Theoretical graph of partially overlapping bimodal

Third, the serious overlap of the bimodal. The two peaks overlap completely and only one peak can be seen on the time spectrum.

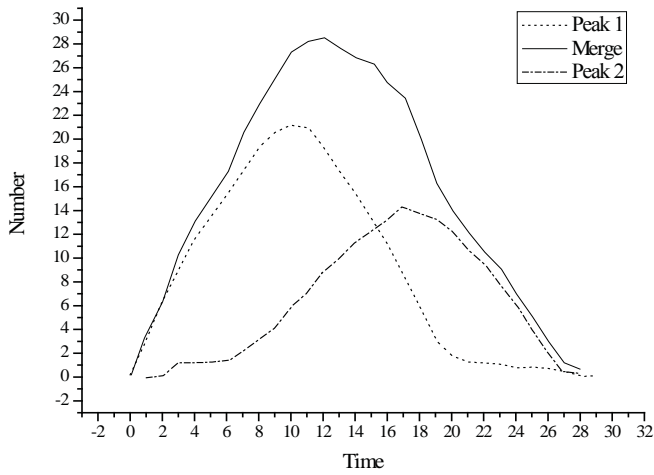


Fig. 3. Theoretical graph of seriously overlapping bimodal

BASIC FUNCTIONS OF THE SOFTWARE

The pulse neutron oxygen activation logging interpretation software is divided into three parts, namely, point measurement calculation, comprehensive calculation and profile result table generation, and result image electronic picture output and printing. The point measurement calculation is used to perform peak identification and flow calculation for a single measurement point. The software can display the measurement data of seven probes at the same time and can filter each curve. The flow rate in the tubing, inside the casing and the oil collar annulus of each peak is calculated.

The flow value of the measurement point is imported into the comprehensive calculation section. Combined with the perforation horizon, water distributor, packer, bell mouth and other structural positions, the suction profile is calculated, and the results graph and the results table data are produced. It also includes a carbon dioxide flooding calculation module and a single point calculation module. The density and mass flow of carbon dioxide are calculated [14]. The single point calculation module enables the mutual conversion of time, flow rate and flow for a specific source distance, which is used as a reference in identifying peaks.

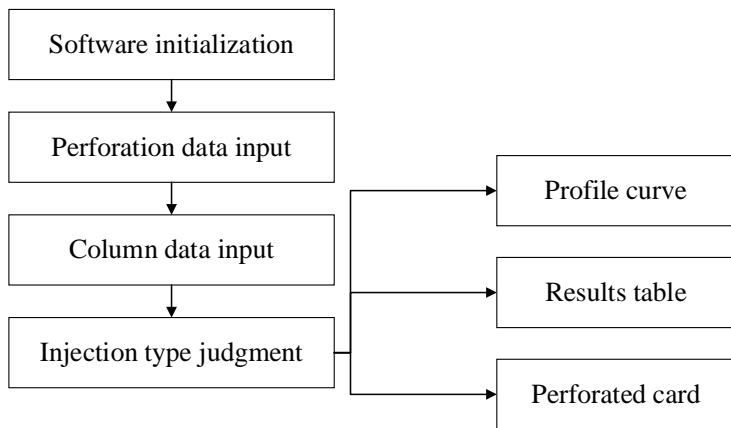


Fig. 4. Flowchart of integrated computation

The software first judges whether the water injection is positive or negative injection, compounding, general injection or double pipe layering according to the perforation interval and column structure data (water distributor, packer, bell mouth). The point flow data is imported to calculate the amount of injection for each layer. Finally, the injection profile curve (tubing flow profile, casing flow profile, reverse injection annulus profile, up flow and downflow separation), outcome data, conclusion cards, perforation cards were calculated. The specific process is shown in Figure 4 [15].

The single point calculation module enables the conversion of time, flow rate and flow to a specific source distance. Based on the column data and fluid space type, combined with the source distance, the software converts the three parameters of time, flow rate and flow. In the peak identification process, the time in the graph is determined based on the estimated flow value. The flow rate is determined based on the estimated flow rate and time. During construction, the selection of measurement points and the verification of the validity of the measurement results are guided.

DOUBLE PIPE LAYERED WATER INJECTION

The double-pipe layered water injection method is complicated, which makes the underground water flow form more complicated. To make the interpretation more intuitive, the multi-section form is used to show the interpretation of the results. The flow profile for interpreting the results graph is three lanes. They represent the inner tubing water flow, the tubing annulus water flow and the oil jacket space water flow, respectively.

The peak is determined by the relationship between flow, flow rate and time, as shown in Figure 5. The flow rate is different in different column structures. It is converted to time based on the distance between the neutron tube and the detector (source distance) [16]. According to the relationship between flow and time, the peak is judged. This method is generally used to determine the peak position of the total injected amount. In the double-tube stratified injection well, the peak position of the total water flow in the oil pipe, the oil pipe annulus and the oil jacket annulus can be judged, which provides a reference for determining the flow peaks of each layer in the next step.

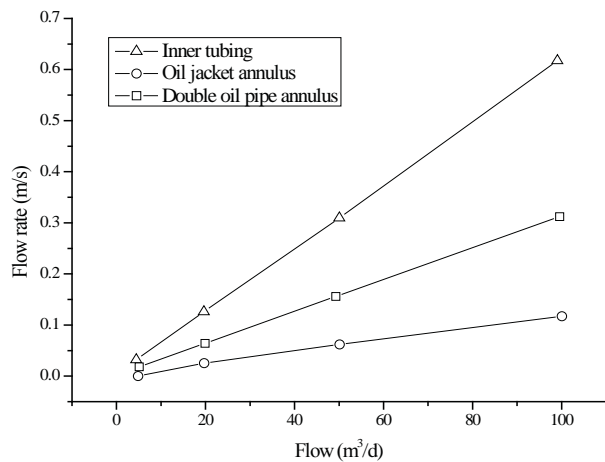


Fig. 5. The relationship between inner tubing, oil jacket annulus and double oil pipe annulus

Tab. 1. Log interpretation results

Layer number	Perforating section (m)	Relative water absorption (%)	Absolute water absorption (m ³ /d)	Degree of water absorption (m ³ /d/m)	Flow direction
12	1665.0-1669.9	6.68	3.21	0.68	Oil jacket up
13	1670.4-1678.9	14.16	6.81	1.49	Oil jacket up
		17.09	8.21	2.17	Oil jacket up
15	1684.0-1694.9	13.12	6.31	1.27	Oil jacket up
		16.05	7.69	1.34	Oil jacket up
16	1695.2-1701.7	6.45	3.09	1.12	Oil jacket up
		10.01	4.81	1.34	Oil jacket up
18	1711.0-1715.9	11.66	5.61	1.18	Oil jacket up
19	1716.6-1723.5	4.79	2.29	0.69	Oil jacket up
Total		100.00	48.03		

Tab. 2. Interpretation results of back injection logging

Layer number	Perforating section (m)	Relative water absorption (%)	Absolute water absorption (m ³ /d)	Degree of water absorption (m ³ /d/m)	Flow direction
25	2140.0-2153.0	-	Not absorbing	-	-
26	2180.0-2196.0	8.08	8.31	1.12	Oil jacket down
		91.92	94.49	11.13	Oil jacket down
27	2224.0-2228.9	-	Not absorbing	-	-
28	2228.9-2230.0	-	Not absorbing	-	-
29	2236.0-2252.0	-	Not absorbing	-	-
30	2258.0-2270.9	-	Not absorbing	-	-
31	2270.9-2280.0	-	Not absorbing	-	-

Tab. 3. Interpretation results of positive logging

Layer number	Perforating section (m)	Relative water absorption (%)	Absolute water absorption (m ³ /d)	Degree of water absorption (m ³ /d/m)	Flow direction
25	2140.0-2153.0	-	Not absorbing	-	-
26	2180.0-2196.0	-	Not absorbing	-	-
27	2224.0-2228.9	26.35	10.81	1.81	Oil jacket up
28	2228.9-2230.0				
29	2236.0-2252.0	5.35	2.19	0.64	Oil jacket up
		-	Not absorbing	-	-
30	2258.0-2270.9	2.45	1.01	0.26	Oil jacket up
		4.86	1.99	0.19	Oil jacket up
		40.99	16.81	4.55	Oil jacket up
31	2270.9-2280.0	15.60	6.39	1.20	Oil jacket up
		4.40	1.81	0.50	Oil jacket up

FIELD APPLICATION

The well depth is 1967.86m. The outer diameter of the casing is 139.7 mm and the outer diameter of the oil pipe is 73 mm. The target layer measurement section is 1630.0-1727.0m, and the daily water injection volume is 48.0 m³/d. The oil pressure is 8.0 MPa and the casing pressure is 0.0 MPa. The single oil pipe is used for general water injection, and the bell mouth is located at 1719.6 m, which is injected into the water and returned to each suction layer. The amount of inhalation at each horizon was determined by pulsed neutron oxygen activation logging. The water absorption of each layer is shown in Table 1.

The well depth of the well is 2490.02 m. The outer diameter of the casing is 177.8 mm and the outer diameter of the oil pipe is 73 mm. The target layer measurement section is 2020.0–2281.0 m, and the daily water injection volume is 120.2m³/d. The oil pressure is 23.5 MPa and the casing pressure is 19.5 MPa. Water is injected by means of oil sleeve. The packer position is 2207.0 m and the bell mouth position is 2300.0 m. According to the pulsed neutron oxygen activation logging, the total injection of the oil jacket annulus is 102.8 m³/d, and the total injection volume of the oil pipeline is 41.0 m³/d. The amount of inhalation of each layer is determined. The water absorption of each layer is shown in Table 2.

CONCLUSION

Aiming at the actual logging data of offshore oilfields, the interpretation methods are studied, including spectral peak identification feature analysis methods and interpretation model establishment. In particular, the spectral peak identification method and carbon dioxide flooding interpretation method for double-tube layered water injection are proposed. Oxygen activation logging can be implemented in oil fields. This interpretation method basically meets the existing logging requirements.

For the test design and interpretation method of the research, the corresponding interpretation software is written. The software includes point measurement calculation, comprehensive calculation, profile result table generation and electronic picture output and printing. After a period of practical application, this method has undergone a series of improvements. At present, the actual interpretation needs have been met. As the application deepens and the scope of application expands, the software needs to be continuously improved and expanded.

REFERENCES

1. C. Qing, X. Wu, X. Li, W. Zhu, C. Qiao, and R. Rao, *Use of weather research and forecasting model outputs to obtain near-surface refractive index structure constant over the ocean*, Optics Express, Vol. 24, No. 12, pp. 13303–13315, 2016.
2. M. Wang, X. Liu, L. Tan, L. Jiang S. Seunghyun, and S. Wei, *Impacts of viirs sdr performance on ocean color products*, Journal of Geophysical Research-atmospheres, Vol. 118, No. 18, pp. 10347–10360, 2016.
3. A. Camps, J. Font, M. Vall-Llossera, I. Corbella N. Duffo, and F. Torres, *Determination of the sea surface emissivity at l-band and application to smos salinity retrieval algorithms: review of the contributions of the upc-icm*, Radio Science, Vol. 43, No. 3, pp. 1–16, 2016.
4. W. D. Robinson, B. A. Franz, J. H. Ahn, and J. H. Ahn, *Cloud motion in the goci/coms ocean colour data*, International Journal of Remote Sensing, Vol. 37, No. 20, pp. 4948–4963, 2016.
5. R. H. Morin, G. E. Descamps, and L. D. Cecil, *Acoustic televiewer logging in glacier boreholes*. Journal of Glaciology, Vol. 46, No. 46, pp. 695–699, 2017.
6. W. S. Chan, M. L. Mah, R. C. Bay, and J. J. Talghader, *Long-wavelength optical logging for high-resolution detection of ash layers in glacier ice* Journal of Glaciology, Vol. 63, No. 237, pp. 17–21, 2016.
7. G. C. Hays, L. C. Ferreira, A. M. M. Sequeira, M. G. Meekan, C. M. Duarte, and H. Bailey, *Key questions in marine megafauna movement ecology*, Trends in Ecology & Evolution, Vol. 31, No. 6, pp. 463–475, 2016.
8. B. C. Bennett, *The sound of trees: wood selection in guitars and other chordophones*, Economic Botany, Vol. 70, No. 1, pp. 49–63, 2016.
9. S. Biancamaria, D. P. Lettenmaier, and T. M. Pavelsky, *The swot mission and its capabilities for land hydrology*, Surveys in Geophysics, Vol. 37, No. 2, pp. 307–337, 2016.
10. M. Glasius, and A. H. Goldstein, *Recent discoveries and future challenges in atmospheric organic chemistry*, Environmental Science & Technology, Vol. 50, No. 6, pp. 2754, 2016.
11. S. Kasim, N. A. Omar, N. S. Mohammad Akbar, R. Hassan, and M. A. Jabar, *Comparison Semantic Similarity Approach Using Biomedical Domain Dataset*, Acta Electronica Malaysia, Vol. 1, No. 2, pp. 1–4, 2017.
12. N. S. Ismail, S. Kasim, Y. Y. Jusoh, R. Hassan, and A. Alyani, *Medical Appointment Application*, Acta Electronica Malaysia, Vol. 1, No. 2, pp. 5–9, 2017.
13. Z. He, X. Gu, X. Y. Sun, J. Liu, and B. S. Wang, *An Efficient Pseudo-Potential Multiphase Lattice Boltzmann Simulation Model for Three-Dimensional Multiphase Flows*, Acta Mechanica Malaysia, Vol. 2, No. 1, pp. 01–03, 2018.
14. X. Luo, *Research on Anti-Overturning Performance Of Multi-Span Curved Girder Bridge with Small Radius*, Acta Mechanica Malaysia, Vol. 2, No. 1, pp. 04–07, 2018.
15. H. Farrajia, N. Qamaruzaman, S. K. Md Sa'ata, and A. F. Dashtia, *Phytoremediation of suspended solids and turbidity of palm oil mill effluent (POME) by Ipomea aquatic*, Engineering Heritage Journal, Vol. 1, No. 1, pp. 36–40, 2017.
16. F. De'nan, H. Hasan, and M. Mahzuz, *Behaviour of the beam to column connection for tapered steel section with perforation*, Engineering Heritage Journal, Vol. 1, No. 1, pp. 41–44, 2017.

CONTACT WITH THE AUTHORS

**Caiyun Gu
Peng Zhao
Li Wang
Hongxia Guo**

Yulin University
Shaanxi 719000
CHINA